www.czasopisma.pan.pl PAN www.journals.pan.pl

ARCHIVE OF MECHANICAL ENGINEERING

DOI: 10.24425/ame.2026.157603 2026, Vol. 73, No. 1, pp. 79–101

Chitra KUMAR [1], Krishna Prasad MADASU [1]

Impact of magnetic field and permeability on the unsteady slow rotation of a sphere: slip condition

Received 6 October 2025, **Revised** 1 December 2025, **Accepted** 21 December 2025, **Published online** 21 January 2026

Keywords: rotation, sphere, slip, permeability, Lorentz force, Laplace transform

This study investigates the unsteady rotational motion of a solid spherical particle with slip at its surface, immersed in an incompressible viscous fluid saturating a porous medium, under the influence of an external magnetic field. The flow dynamics are governed by the unsteady Brinkman equation coupled with the Lorentz force. To obtain analytical expressions, the Laplace transform technique is employed, and a slip boundary condition is applied at the surface of the sphere. The torque acting on the sphere is derived in the Laplace domain. The combined influence of the permeability, magnetic field, and slip condition on the torque is examined for three distinct cases: damping oscillatory motion, accelerating velocity, and impulsive motion. Graphical representations are provided to illustrate the variation of torque with time for different values of the Hartmann number, slip parameter, and permeability parameter. The results demonstrate that the Hartmann number and slip parameter enhance the torque in all cases, while the torque decreases with increasing value of the permeability parameter. In the limiting cases, the present results reduce to earlier findings in the absence of magnetic effect and permeability.

1. Introduction

The unsteady rotational motion of a rigid spherical particle in a Brinkman medium provides valuable insights into transport processes in porous and complex fluid environments. The Brinkman model, which generalizes Darcy's law by including viscous shear effects, captures both the permeability of the porous medium and the hydrodynamic interactions near the particle surface [1, 2]. When a magnetic field is applied, additional Lorentz forces act on the conducting or

✉ Krishna Prasad MADASU: madaspra.maths@nitrr.ac.in; kpm973@gmail.com

[1]Department of Mathematics, National Institute of Technology, Raipur, Chhattisgarh, India. Emails: ckumar.phd2024.maths@nitrr.ac.in; chitrakumarsinha8493@gmail.com

magnetizable particle, altering its torque response and rotational [3]. The analysis becomes more comprehensive when the particle surface obeys a velocity slip condition, which represents situations in which the fluid does not adhere perfectly to the particle boundary due to rarefied effects, a polymer coating, or micro-scale interfacial properties. Together, these factors determine how quickly and efficiently the particle responds to applied fields in time-dependent flows.

Such a framework is highly relevant for microscale and biomedical applications, where particles often encounter porous surroundings, magnetic control, and partial slip at fluid–solid interfaces. The transient rotational response not only reflects the combined effects of medium permeability, magnetic field strength, and slip length but also provides a basis for optimizing particle manipulation in technologies such as targeted drug delivery, magnetic separation, and lab-on-a-chip devices. By studying the unsteady regime, one can predict both the short-time inertial effects and the long-time approach to steady motion, thereby offering a comprehensive picture of particle dynamics in realistic complex environments.

Studying the unsteady rotation of spherical particles involves understanding how time-varying angular velocity is affected by slip velocity and transient fluid-particle interactions, with added complexity when magnetic forces are present in the porous medium. In contrast to this study, Srinivasacharya and Prasad [4, 5] investigated the steady rotational motion of a composite and an approximate sphere in a bounded medium and evaluated the formula for the torque. Similarly, Ashmawy [6, 7] studied the unsteady rotational dynamics of a sphere with slip at the particle surface, deriving the torque in both viscous and couple-stress fluids. Sarkar and Madasu [8] examined the impact of couple stresses and slip on the steady rotating sphere in the Brinkman model. Kumar and Madasu [9] recently explored the time-dependent rotational behavior of a rigid spherical particle in a Jeffrey fluid, focusing on how the slip parameter and the Jeffrey fluid's parameters affect the torque acting on the sphere. Chou and Keh [10] analyzed the steady flow induced by a spherical particle rotating in an incompressible Newtonian fluid, confined within an eccentric spherical cavity with slip boundaries along their common diameter at low Reynolds numbers. Building on this, Li and Keh [11] examined the unsteady rotational motion of a spherical particle subjected to a suddenly applied constant torque inside a concentric spherical cavity with slip surfaces. They derived an analytical solution for its transient angular velocity. Their results demonstrated that both the slip conditions at the cavity boundaries and the particle-to-cavity size ratio play a crucial role in governing the particle's rotational dynamics and its time-dependent angular acceleration. Recently, Ayman et al. [12] investigated the transient slow rotation of a spherical particle within a concentric spherical cavity filled with a Brinkman porous medium, considering slip surfaces at both particle and cavity walls. Using the Laplace transform to solve the unsteady Brinkman equations, their study highlighted the roles of permeability, particle-to-cavity radius ratio, slip coefficients, and density ratio in controlling angular motion, with applications in biological fluids, protein transport, and filtration technologies.

The earliest studies of magnetic effects on rotating spherical particles likely stem from classical works in magnetohydrodynamics (MHD) and electromagnetic theory. Maxwell's equations laid the foundation for understanding the interaction between electric and magnetic fields. His theoretical framework forms the basis for studying magnetic effects on moving and rotating bodies [13]. Hartmann's [14] pioneering studies on the behavior of conducting fluids in magnetic fields, particularly the Hartmann flow, established the field of magnetohydrodynamics. These studies are indirectly related to the effects of magnetic fields on rotating particles. Chester [15] examined the electromagnetic forces' impact on the flow of viscous, electrically conductive fluids at low Reynolds numbers while researching the magnetic field's effect on Stokes flow. Blerkom [16] calculated the force acting on the sphere for a range of conductivities and Reynolds numbers while studying the movement of a viscous and electrically conducting fluid around a sphere. Using the Oseen approximation, Gotoh [17] and Goldsworthy [18] subsequently studied the movement of an incompressible, viscous fluid past a sphere when a constant magnetic field runs parallel to the uninterrupted flow.

Swarup and Sinha [19] studied magnetohydrodynamic flow past the sphere and found that a magnetic field affects the drag. Singh and Kumar [20] analyzed the Couette flow of an electrically conducting fluid between two parallel plates under impulsive and uniformly accelerating motion in a uniform transverse magnetic field. Their findings indicate that the magnetic field enhances the velocity field in both cases. Seth and Ghosh [21] investigated the unsteady hydromagnetic flow of an incompressible, viscous, electrically charged fluid in a channel that is rotating when subjected to a periodic pressure gradient and an angled magnetic field. They discovered that the magnetic field's inclination significantly impacts the velocity profiles and skin friction, and that the rotation parameter and magnetic field inclination are essential for regulating the flow characteristics.

Later, Kythe and Puri [22] researched the effects of the induced magnetic field, determining that it alters the velocity of the faster wave but has no influence on the slower wave. Hayat et al. [23] discussed the unsteady magnetohydrodynamics flow resulting from the rotation of a noncoaxial porous disk and a fluid at infinity. Their study revealed that the boundary-layer thickness decreases with increasing magnetic parameter in cases involving suction or blowing. Siddiqui et al. [24] determined precise solutions in magnetohydrodynamic rotating flow. Their paper is connected with the non-torsionally generated time-dependent hydro-magnetic flow within an endless, non-conducting porous disk enclosing a semi-infinite region of a rotating viscous fluid that conducts electricity. Shekhar et al. [25] investigated magnetohydrodynamic flow around a sphere and examined the magnetic effect on the flow.

Kythe and Puri [26] analyzed time-dependent free-convective flows close to an endless perpendicular plate in a rotating medium under a constant transverse magnetic field. In a variety of contexts, Chandrashekhar [27] significantly advanced the theory of hydrodynamic and hydromagnetic flow phenomena. He emphasized the significance of the Coriolis force in problems involving viscous-flow stability and thermal instability in the presence of an external MHD field. Puri and Kulshrestha [28] examined the flow of a three-dimensional viscous fluid in a rotating medium influenced by a transverse magnetic field as it passes through an infinite porous plate with a time-varying velocity, and examined how the flow is affected by suction and the magnetic field.

In 1996, Solomentsev and Anderson calculated the hydrodynamic torque acting on a sphere in a Brinkman fluid. Geindreau and Auriault [29] rigorously derived a tensorial filtration law coupling mass flow and electric current in porous media under magnetic fields, extending Darcy's law with an electric field term and a permeability tensor exhibiting a Hall effect analogue. Saxena and Srivastava [30] investigated the rotational motion of a solid spherical particle in a viscous fluid within a bounded porous medium, while Saxena and Agarwal [31] explored the influence of magnetic fields on the rotation of a sphere. Das et al. [32] studied unsteady magnetohydrodynamic (MHD) Couette flow in a rotating system, deriving exact solutions to the governing equations using the Laplace transform. Seth et al. [33] examined the combined effects of rotation and magnetic fields on unsteady Couette flow through a porous channel, analyzing the behavior of a viscous conducting fluid under a uniform transverse magnetic field. More recently, Premlata and Wei [34] presented a theoretical analysis of axisymmetric stick–slip Janus particles (SSJP) under creeping flow, revealing behaviors distinct from those of no-slip or uniform-slip particles. Their findings highlighted a constant torque plateau at small stick-face coverage and a reduced Basset torque decaying as $\frac{1}{\delta}$ (where δ is the Stokes boundary layer thickness) due to the slip face. Their results offer fresh insights into the behaviour of Janus particles and potential manipulation techniques.

Nagaraju et al. [35] and Madasu and Bucha [36] investigated magnetohydrodynamic (MHD) effects on rotating free-surface flows of micropolar fluids in porous-lined cylindrical containers, as well as the influence of magnetic fields on the slow motion of porous spheroids within the Brinkman framework. Subsequently, Madasu and Bucha [37, 38] analyzed the dynamics of a viscous fluid sphere enclosed in a spherical shell, focusing on the impact of magnetic fields on the creeping motion of porous spheroids. Their studies further addressed Brinkman-type modeling and MHD effects on the motion of micropolar fluids around spherical bodies embedded in porous media. El-Sapa and Altudais [39] considered the influence of a transverse magnetic field on the flow around two rigid spheres in porous media with slip boundaries, while El-Sapa [40] examined the combined roles of magnetic fields and slip on the motion of a rigid sphere in a viscous fluid. The rotational motion of a magnetohydrodynamic couple stress fluid between concentric spheres with slip at the inner boundary has been studied by Al-Hanaya and El-Sapa [41], where analytical solutions reveal the influence of magnetic field, couple stress parameters, and slip on torque behavior, along with reductions in the wall correction factor. More recently, Alotaibi and El-Sapa [42] explored the magnetohydrodynamic characteristics of couple-stress fluids under slip conditions between concentric spheres.

Several recent studies by Yadav et al. [43] and Yadav and Roshan [44–47] have contributed significantly to understanding peristaltic and unsteady non-Newtonian fluid flows in physiological and biomedical contexts. Their work encompasses a variety of complex flow models, including the Jeffrey and biviscosity fluids, to simulate blood flow through stenosed or flexible arteries and annular geometries under the influence of body acceleration, electromagnetic fields, and wall-slip effects. Using analytical and semi-analytical techniques, such as the perturbation and homotopy perturbation methods, they derived expressions for key flow characteristics, including velocity, wall shear stress, pressure gradient, impedance, and trapping phenomena. Their analyses reveal how parameters like the Hartmann number, inclination angle, permeability, amplitude ratio, and phase difference influence the flow, heat transfer, and mechanical efficiency in peristaltic transport. Moreover, through comparative studies of sinusoidal, triangular, trapezoidal, and square waveforms, they provided insight into fluid–structure interactions and the optimization of peristaltic endoscope designs for medical and mechanical applications. Collectively, these investigations form a comprehensive foundation for studying electromagnetohydrodynamic and non-Newtonian flows in deformable conduits, offering strong motivation for extending such analyses to more complex unsteady or electrokinetic systems.

Based on the above literature survey and to the best of the authors' knowledge, the effects of the Hartman number with permeability parameter on the torque experienced by the fluid on a unsteady rotating slip sphere have not yet been investigated. In this paper, we investigated the time-dependent rotational motion of a rigid spherical particle immersed in an incompressible Newtonian fluid within a porous medium in the presence of an external magnetic field. The torque acting on the spherical surface is derived in the Laplace domain for various parameter regimes, with particular emphasis on the influence of the magnetic field, the permeability parameter, and slip effects. To gain further insight, the torque is numerically evaluated for three distinct cases of time-dependent fluid motion. The results are presented in graphical illustrations that highlight the combined effects of magnetic field strength, porous medium permeability, and a slip condition on the unsteady torque response. The current study focuses on systems that utilize magnetically controlled rotation of micro- or nano-sized spherical particles suspended in electrically conductive or partially permeable fluids. Applications of this technology include microfluidic lab-on-chip devices, magnetic bead-based biochemical separations, and targeted drug delivery [48–50].

2. Formulation of the problem

Consider a solid sphere of radius "a" immersed in an incompressible viscous fluid that saturates a porous medium (see Fig. 1). Initially, both the fluid and the sphere are at rest. The sphere is suddenly set into rotation around an instantaneous axis with an angular velocity that changes with time, denoted as "$\Omega_0 V(t)$", where

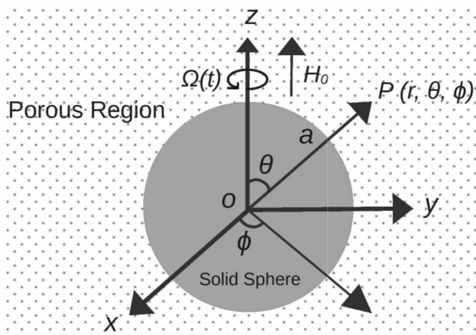

Fig. 1. Geometrical sketch of the problem

Ω_0 is a constant with the dimensions of angular velocity and $V(t)$ is a dimensionless function of time. The following assumptions are made in this study:

1. The flow is axisymmetric, slow, and unsteady.
2. The body force is absent.
3. A uniform constant magnetic field is applied in a transverse direction of the flow.
4. We assume that the magnetic Reynolds number $Re_m = \Omega_0 a^2 \mu_h \sigma$ is very small. Where μ_h: magnetic permeability and σ: electrical conductivity.
5. Any applied external field is excluded.
6. The induced magnetic field is neglected.

The motion of the electrically conductive, incompressible, viscous fluid is controlled by the conservation laws of mass and momentum equations, which govern the magnetohydrodynamic (MHD) flow [16]. The fluid is assumed to have constant properties for its electrical conductivity.

The Lorentz force $\vec{F}_L$ is presented by [3]

$$\vec{F}_L = \mu_h(\vec{J} \times \vec{H}), \tag{1}$$

where $\vec{H}$ is magnetic induction, and $\vec{j}$ is electric current density, which is given by Ohm's law [3] as

$$\vec{j} = \sigma\left(\vec{E} + \mu_h \vec{q} \times \vec{H}\right). \tag{2}$$

Here $\vec{q}$ means velocity vector of the fluid.

Consider a uniform magnetic field is applied in the transverse direction of the flow, i.e., $\vec{H} = H_0\,\vec{e}_r$. The magnetic Reynolds number is assumed to be very small, and there is no external electric field; therefore, the induced current is also very small. Consequently, we consider the induced electric field and the induced magnetic field to be negligible, so that Eq. (1) can be written as [3, 51]

$$\vec{F}_L = \sigma\mu_h^2(\vec{q} \times \vec{H}) \times \vec{H}. \tag{3}$$

The governing equation for the unsteady creeping motion of an incompressible Newtonian fluid in the porous medium with the presence of the Lorentz force term can be expressed by [29]

$$\nabla \cdot \vec{q} = 0, \tag{4}$$

$$\rho \frac{\partial \vec{q}}{\partial t} = -\nabla p + \mu \nabla^2 \vec{q} - \frac{\mu}{k} \vec{q} + \sigma \mu_h^2 (\vec{q} \times \vec{H}) \times \vec{H}, \tag{5}$$

where: ρ – density, p – pressure, μ – dynamic viscosity coefficient, k – permeability of the porous medium, and ∇ – Hamiltonian "nabla" operator.

Representation of the stress tensor is

$$t_{ij} = -p\delta_{ij} + 2\mu e_{ij}, \quad \text{with} \quad e_{ij} = \frac{1}{2} \left(q_{i,j} + q_{j,i} \right). \tag{6}$$

Here: comma (,) denotes the partial differentiation, t_{ij} is the component of shear stress which is normal along i and in the direction j, e_{ij} is the rate of strain, and the Kronecker delta δ_{ij} is presented by

$$\delta_{ij} = \begin{cases} 1 & \text{if } i = j, \\ 0 & \text{if } i \neq j. \end{cases} \tag{7}$$

Using the spherical polar coordinates (r, θ, ϕ) with the origin located at the center of the sphere, the fluid velocity vector and magnetic field, which is applied in the transverse direction of the flow, are assumed to take the following form

$$\vec{q}(r, \theta, t) = q_\phi(r, \theta, t)\, \vec{e}_\phi. \tag{8}$$

We assume that the flow is incompressible and axisymmetric. The velocity field has only the azimuthal component q_ϕ, and there is no motion in the r and θ directions, so there is no pressure gradient driving the azimuthal flow, and it does not contribute to the rotation. By this assumption, Eq. (5) reduces to

$$\rho\, s\, \bar{q}_\phi(r, \theta, s) = \mu E^2\, \bar{q}_\phi\,(r, \theta, s) - \frac{\mu}{k} \bar{q}_\phi\,(r, \theta, s) - \sigma \mu_h^2 H_0^2 \bar{q}_\phi\,(r, \theta, s), \tag{9}$$

where the overhead bar on the velocity vector indicates the Laplace transform, and "E^2" represents the Stokesian differential operator, which are defined by

$$\bar{f}(s) = \int_0^\infty e^{-st} f(t) \mathrm{d}t, \tag{10}$$

$$E^2 = \frac{\partial^2}{\partial r^2} - \frac{\cot\theta}{r^2} \frac{\partial}{\partial \theta} + \frac{1}{r^2} \frac{\partial^2}{\partial \theta^2}. \tag{11}$$

The initial condition of the fluid velocity takes the following form:

$$q_\phi(r, \theta, 0^+) = \begin{cases} \Omega(0) a \sin\theta, & \text{for } \; r = a \\ 0, & \text{for } \; r > a. \end{cases} \tag{12}$$

The solid sphere's surface is subjected to the slip boundary condition listed below [6, 7]:

$$\beta\left\{q_\phi(a,\theta,t)-\Omega(t)\,r\sin\theta\right\}=t_{r\phi},\qquad r=a,\qquad t>0. \tag{13}$$

Here: β – slip coefficient and $t_{r\phi}$ – shear stress, which is normal along r in the ϕ direction.

We require some non-dimensional variables to make our governing equation dimensionless, which are as follows [2, 9]

$$\tilde{r}=\frac{r}{a},\quad \tilde{\vec{q}}=\frac{\vec{q}}{a\Omega_0},\quad \tilde{E}^2=a^2E^2,\quad \tilde{\Omega}(t)=\frac{\Omega(t)}{\Omega_0},\quad \text{and}\quad \tilde{t}_{r\phi}=\frac{t_{r\phi}}{\mu\,\Omega_0}. \tag{14}$$

By the assumption (8) and dimensional scheme (14), the Eq. (9) will be reduce in the following form

$$(E^2-\Lambda^2)\,r\,\sin\theta\,\bar{q}_\phi(r,\theta,s)=0. \tag{15}$$

Here, the expression of the notation Λ^2 is following

$$\Lambda^2=\alpha^2+\frac{a^2s}{\nu}+\xi^2, \tag{16}$$

where permeability parameter $\alpha=\sqrt{\dfrac{a^2}{k}}$, Hartman number $\xi=\sqrt{\dfrac{\sigma\mu_h^2H_0^2a^2}{\mu}}$, and kinematic viscosity $\nu=\dfrac{\mu}{\rho}$.

From dimensionless scheme (14) for the boundary condition (13), takes the following form

$$\beta_1\left\{q_\phi(r,\theta,t)-\Omega(t)\,r\sin\theta\right\}=t_{r\phi},\qquad r=1\ \text{ and }\ t>0. \tag{17}$$

Here $\beta_1=\dfrac{a\beta}{\mu}$ is a dimensionless slip parameter, which is referred to as the Navier number, which measures the degree of tangential slip between the fluid and the boundary. When $\beta_1\to\infty$, it corresponds to the classical no-slip situation, which will be derived as a special case in this paper.

3. Solution of the problem

The solution of Eq. (15) is [52]

$$\bar{q}_\phi(r,\theta,s)=\frac{1}{\sqrt{r}}\left(AK_{\frac{3}{2}}(\Lambda r)+BI_{\frac{3}{2}}(\Lambda r)\right)\sin\theta. \tag{18}$$

Here, $K_{\frac{3}{2}}(\Lambda r)$ and $I_{\frac{3}{2}}(\Lambda r)$ are modified Bessel functions of order $3/2$, since $\bar{q}_\phi(r,\theta,s)$ should be finite as $r \to \infty$, so we have $B = 0$ so this implies

$$\bar{q}_\phi(r,\theta,s) = A\sqrt{\frac{\pi}{2\Lambda}}e^{-\Lambda r}\left(\frac{1}{r} + \frac{1}{\Lambda r^2}\right)\sin\theta. \tag{19}$$

Taking the Laplace transform of boundary condition (17) gives the value of coefficient A, i.e.,

$$A = \frac{\beta_1\,\bar{\Omega}(s)\,\Lambda\,e^{\Lambda}}{\sqrt{\dfrac{\pi}{2\Lambda}}\,\left(\Lambda^2 + (\beta_1+3)(\Lambda+1)\right)}. \tag{20}$$

Now, substituting the value of A into Eq. (19) we get the velocity of the fluid as follows

$$\bar{q}_\phi(r,\theta,s) = \frac{\beta_1\,\bar{\Omega}(s)\,\Lambda\,e^{-\Lambda(r-1)}\left(\dfrac{1}{r} + \dfrac{1}{\Lambda r^2}\right)\sin\theta}{\Lambda^2 + (\beta_1+3)(\Lambda+1)}. \tag{21}$$

The Laplace transform of shear stress $t_{r\phi}$ for a viscous fluid will be

$$\bar{t}_{r\phi} = -\frac{\mu\,\beta_1\bar{\Omega}(s)}{\Lambda^2 + (\beta_1+3)(\Lambda+1)}\left(\frac{\Lambda^2}{r} + \frac{3\Lambda}{r^2} + \frac{3}{r^3}\right)e^{-\Lambda(r-1)}\sin\theta. \tag{22}$$

In the domain of the Laplace transform, the torque operating on the solid sphere can be obtained by [2, 12]

$$\bar{T} = 2\pi a^3\int_0^\pi r^3\,\bar{t}_{r\phi}\big|_{r=1}\,\sin^2\theta\,\mathrm{d}\theta. \tag{23}$$

The simplified version of Eq. (23) is the following:

$$\bar{T} = -\frac{8\pi a^3\mu\beta_1}{\beta_1+3}\left(\bar{\Omega}(s) + \frac{\beta_1\Lambda^2\bar{\Omega}(s)}{3\left(\Lambda^2 + (\beta_1+3)(\Lambda+1)\right)}\right). \tag{24}$$

From Eq. (16) and Eq. (24), the final torque formula of this study in the Laplace domain is

$$\bar{T} = -\frac{8\pi a^3\mu\beta_1}{\beta_1+3}\left(\bar{\Omega}(s) + \frac{\beta_1\bar{\Omega}(s)\left(\alpha^2 + \dfrac{a^2 s}{\nu} + \xi^2\right)}{3\left(\alpha^2 + \dfrac{a^2 s}{\nu} + \xi^2 + (\beta_1+3)\left(1 + \sqrt{\alpha^2 + \dfrac{a^2 s}{\nu} + \xi^2}\right)\right)}\right). \tag{25}$$

Put $\xi = 0$ in Eq. (25), it gets the torque formula for the case of a rotating sphere in a porous medium.

$$\bar{T} = -\frac{8\pi a^3 \mu \beta_1}{\beta_1 + 3}\left(\bar{\Omega}(s) + \frac{\beta_1 \bar{\Omega}(s)\left(\alpha^2 + \frac{a^2 s}{\nu}\right)}{3\left(\alpha^2 + \frac{a^2 s}{\nu} + (\beta_1 + 3)\left(1 + \sqrt{\alpha^2 + \frac{a^2 s}{\nu}}\right)\right)}\right). \tag{26}$$

When $\alpha \to 0$, it will be the case for a clear viscous fluid with the presence of a magnetic field, and the formula for the torque is

$$\bar{T} = -\frac{8\pi a^3 \mu \beta_1}{\beta_1 + 3}\left(\bar{\Omega}(s) + \frac{\beta_1 \bar{\Omega}(s)\left(\frac{a^2 s}{\nu} + \xi^2\right)}{3\left(\frac{a^2 s}{\nu} + \xi^2 + (\beta_1 + 3)\left(1 + \sqrt{\frac{a^2 s}{\nu} + \xi^2}\right)\right)}\right). \tag{27}$$

When $\beta_1 \to \infty$, it will be the case of no-slip, and the formula of the torque in porous medium with the presence of an applied magnetic field is presented as

$$\bar{T} = -8\pi a^3 \mu \left(\bar{\Omega}(s) + \frac{\bar{\Omega}(s)(\alpha^2 + \frac{a^2 s}{\nu} + \xi^2)}{3\left(1 + \sqrt{\alpha^2 + \frac{a^2 s}{\nu} + \xi^2}\right)}\right). \tag{28}$$

When $t \to \infty$, it will be the case for steady rotation of a solid sphere in a viscous fluid filled with a porous medium with constant angular velocity Ω_0, taking into account the effect of the Hartman number

$$\bar{T} = -\frac{8\pi a^3 \mu\, \Omega_0\, \beta_1}{\beta_1 + 3}\left(1 + \frac{\beta_1(\alpha^2 + \xi^2)}{3\left(\alpha^2 + \xi^2 + (\beta_1 + 3)\left(1 + \sqrt{\alpha^2 + \xi^2}\right)\right)}\right). \tag{29}$$

To align with the framework presented in [6], the magnetic field term ξ and non-dimensional permeability parameter of porous medium α have been removed. This ensures a clear comparison and highlights the effect of the primary contributing factors. When the magnetic field and porous medium are absent, i.e., $\xi = 0$ and $\alpha \to 0$

$$\bar{T} = -\frac{8\pi a^3 \mu \beta_1}{\beta_1 + 3}\left(\bar{\Omega}(s) + \frac{\bar{\Omega}(s)\, \beta_1 a^2 s}{3\left(a^2 s + (\beta_1 + 3)\left(\nu + \sqrt{a^2 s \nu}\right)\right)}\right). \tag{30}$$

When the limit $t \to \infty$ is applied in Eq. (25) with $\xi = 0$, the expression for the torque on a slip sphere rotating with a constant angular velocity Ω_0 in a Brinkman medium reduces to the form reported earlier by Madasu and Sarkar [53]

$$T = -\frac{8\pi a^3 \mu \Omega_0 \beta_1}{3} \left(\frac{\alpha^2 + 3\alpha + 3}{\alpha^2 + (\beta_1 + 3)(1 + \alpha)} \right). \tag{31}$$

In the case $t \to \infty$, $\beta_1 \to \infty$, and $\xi = 0$, Eq. (25) yields the torque acting on a rotating sphere in a Brinkman medium under the classical no-slip boundary condition

$$T = -\frac{8\pi a^3 \mu \Omega_0}{3} \left(\frac{\alpha^2 + 3\alpha + 3}{1 + \alpha} \right). \tag{32}$$

This limiting result is in agreement with the formulation given by Solomentsev and Anderson [54].

The inversion of Eq. (25) analytically is a very tough task, so we are using a Laplace inversion technique to invert and get results numerically [55–57].

4. Some examples of unsteady special fluid flows

Case 1: Damping Oscillatory flow
In this case, the sphere is assumed to perform a damping oscillation so that angular velocity is given by the following expression [6]

$$\Omega(t) = \Omega_0 V(t) = \Omega_0 e^{-\omega t} \sin \omega t, \tag{33}$$

where ω is the oscillation angular frequency of the rotating sphere.

Case 2: Accelerating velocity
In this specific case of fluid flow, we consider that the sphere begins to flow with a time-dependent function $V(t) = \omega t$, so the angular velocity takes the form [6]

$$\Omega(t) = \Omega_0 \omega t. \tag{34}$$

Case 3: Sudden motion
In this case, we assume that the sphere starts to rotate suddenly with constant angular velocity. Therefore, $V(t) = H(t)$, where $H(t)$ is the Heaviside unit step function defined by

$$H(t) = \begin{cases} 1, & t > 0, \\ 0, & \text{otherwise}. \end{cases} \tag{35}$$

The angular velocity for this special case is [7]

$$\Omega(t) = \Omega_0 H(t). \tag{36}$$

5. Results and discussion

The non-dimensional torque is determined by

$$T^* = -\frac{T}{8\pi a^3 \mu\, \Omega_0}.$$

In Figs. 2–7, the values of parameters are as follow:

(1) Slip parameter: $0 \leqslant \beta_1 < \infty$ [6, 7].

(2) Permeability parameter: $k_1 \left(= \frac{1}{\alpha} = \frac{\sqrt{k}}{a} \right)$, $0 \leqslant k_1 < \infty$ [4, 12, 38].

(3) Hartman number: $0 \leqslant \xi < \infty$ [58, 59].

(4) Time: $t > 0$, frequency: $\omega = 1$, $a = 1$, and kinematic viscosity: $\nu > 0$.

In Fig. 2, the non-dimensional torque versus dimensionless time is shown for varying Hartmann numbers (ξ), with slip and permeability parameters fixed for case 1, where the sphere oscillates with constant frequency ω. As seen in Fig. 2a, the torque increases with ξ, exhibiting damped oscillations of initially high amplitude that decay to zero over time. Since the Hartmann number characterizes magnetic-field strength, a stronger field introduces additional resistive torque (magnetic braking), requiring greater hydrodynamic torque to sustain the particle's oscillation.

Fig. 2b illustrates the variation of torque with time for different values of the permeability parameter k_1, with $\xi = 1$ and $\beta_1 = 5$ fixed, in the case where the sphere undergoes damped oscillatory motion with angular frequency $\omega = 1$. The results show that the torque decreases slightly as k_1 increases. This behavior arises because the porous matrix partially isolates the sphere from the surrounding fluid. As permeability increases, this isolation becomes more effective, reducing the fluid resistance experienced by the sphere and thereby lowering the torque required to sustain its rotation.

Fig. 2c shows the variation of dimensionless torque with dimensionless time for different values of the slip parameter (β_1) during the damped oscillatory motion of the sphere. The results indicate that the torque increases with increasing β_1. This occurs because slip reduces the effectiveness of fluid entrainment by the sphere: greater slip requires higher torque to maintain the same rotational motion. At $\beta_1 = 0$, corresponding to perfect slip, the fluid slides over the surface with minimal shear, producing very low viscous stress and torque. In contrast, as $\beta_1 \to \infty$ (the no-slip limit), the sphere strongly couples with the fluid, generating a large velocity gradient and high viscous stresses, which lead to a significant increase in torque.

Fig. 3 illustrates the variation of non-dimensional torque with dimensionless time for different values of ξ in case 2. Figs. 3a and 3c show that, in this case, the torque increases linearly with time. They further indicate that both the magnetic field and the slip parameter enhance the torque when the sphere accelerates in

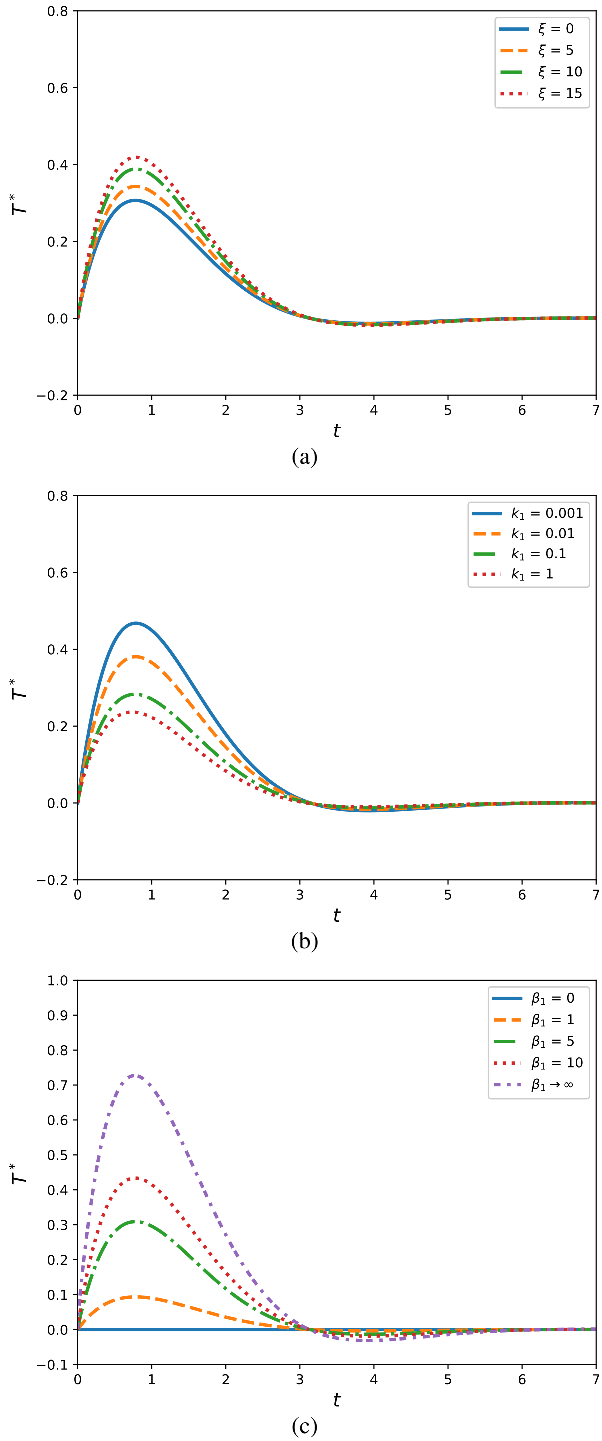

Fig. 2. Variation of dimensionless torque versus time for case 1: (a) with various value of ξ, $\beta_1 = 5$, $k_1 = 0.05$; (b) with various value of k_1, $\beta_1 = 5$, $\xi = 1$; (c) with various value of β_1, $k_1 = 0.05$, $\xi = 1$

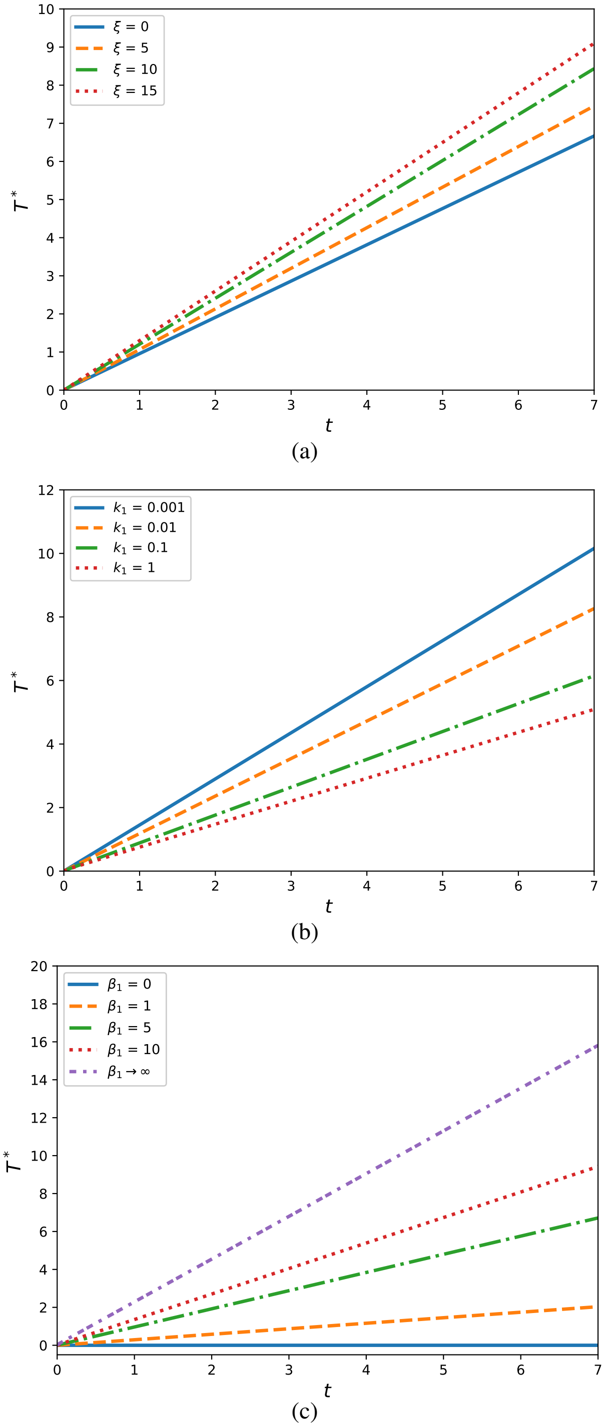

Fig. 3. Plots of dimensionless torque versus time for case 2: (a) with various values of ξ, $\beta_1 = 5$, $k_1 = 0.05$; (b) with various values of k_1, $\beta_1 = 5$, $\xi = 1$; (c) with various values of β_1, $k_1 = 0.05$ $\xi = 1$

the fluid. Fig. 3b presents the variation of torque with time for different values of the permeability parameter, demonstrating that torque decreases as permeability increases.

Fig. 4 presents the variation of dimensionless torque with dimensionless time for different parameter values in case 3, where the sphere undergoes impulsive motion. Figs. 4a and 4c show that the torque initially attains a high value, then decreases with time, and eventually approaches a steady state. These figures also indicate that the torque increases with increasing ξ and β_1. In contrast, Fig. 4b demonstrates that the torque decreases with increasing k_1, which is consistent with the torque expression containing the term $\frac{1}{k_1}$, clearly implying that higher permeability reduces torque.

Fig. 5 depict the effect of permeability (k_1) on the torque acting on a rotating sphere for different values of the slip parameter (β_1), with the Hartmann number (ξ) held constant. As shown in Figs. 5a, 5b, and 5c, the torque increases with β_1 for fixed k_1, indicating that it is a monotonically increasing function of the slip parameter. In the no-slip limit ($\beta_1 \to \infty$), the torque reaches its maximum, while increasing slip (lower β_1) reduces the fluid resistance at the boundary and consequently decreases the torque relative to the no-slip case.

Fig. 6 presents the combined effect of the Hartmann number (ξ) and permeability parameter (k_1) on the torque for the special fluid flow case considered in this study. In Fig. 6a, the variation of torque with ξ and k_1 is shown for fixed values of other parameters during the damped oscillatory motion of the sphere. At low k_1, the porous medium strongly resists fluid motion, leading to a higher torque. As k_1 increases, the medium permits greater fluid penetration, reducing hydrodynamic resistance and consequently lowering the torque. By contrast, the magnetic field introduces a Lorentz force that resists fluid motion and suppresses secondary flows. As ξ increases, this magnetic damping acts as an additional viscous drag, thereby enhancing resistance and increasing the torque required to maintain rotation. Similar trends are observed in Figs. 6b and 6c.

Fig. 7 displays the combined influence of the magnetic field and slip parameter on torque for a fixed permeability of the porous medium. As shown in Figs. 7a, 7b, and 7c, both the Hartmann number (ξ) and slip parameter (β_1) increase the torque in the unsteady rotational motion of the sphere. This occurs because the magnetic field introduces a Lorentz force that resists fluid motion, thereby requiring higher torque to sustain rotation. Similarly, increasing slip weakens the fluid–sphere coupling, so the sphere must exert a greater torque to maintain the same rotational velocity. Together, these effects demonstrate how magnetic and slip conditions significantly influence hydrodynamic resistance in porous media flows.

The study extensively examines the effects of slip, permeability, and the Hartman number on the time-dependent case; however, this current work can be extended to other geometries, including bounded and unbounded media. Future research could also explore the problem under different boundary conditions or by incorporating non-linear terms to gain deeper insights.

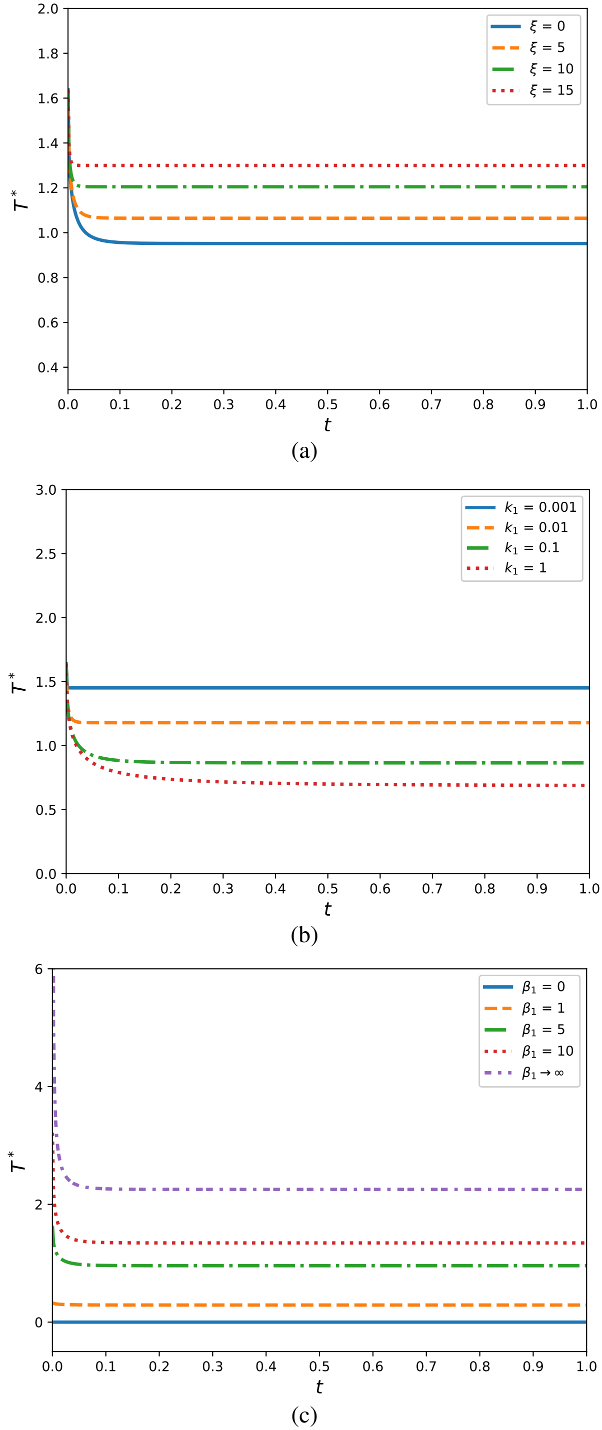

Fig. 4. Variation of non-dimensional torque versus time for case 3: (a) with different values of ξ, $\beta_1 = 5$, $k_1 = 0.05$; (b) with different values of k_1, $\beta_1 = 5$, $\xi = 1$; (c) with different values of β_1, $k_1 = 0.05$, $\xi = 1$

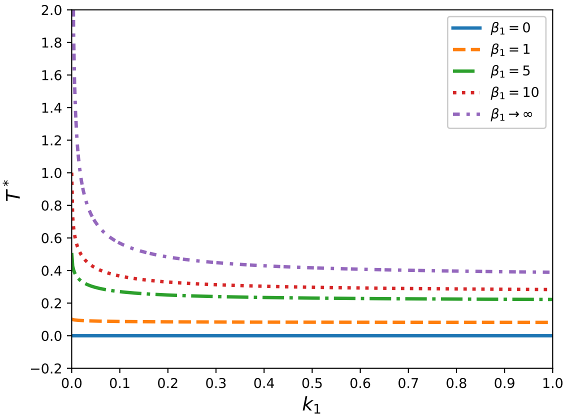

(a)

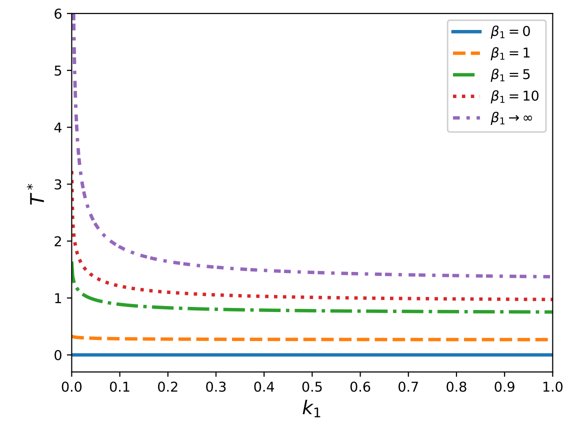

(b)

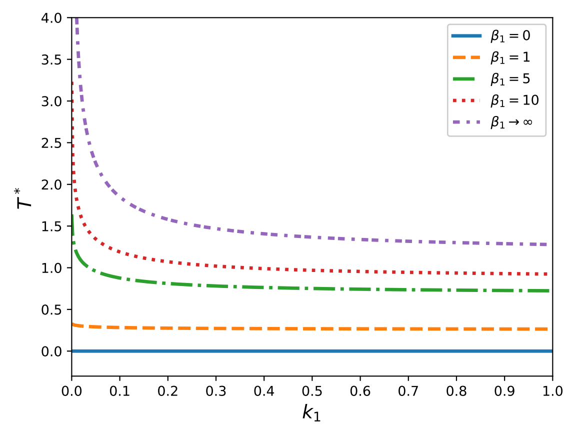

(c)

Fig. 5. Plots of torque versus permeability parameter with different values of β_1: (a) $\xi = 1$, $t = 1$ for case 1; (b) $\xi = 1$, $t = 1$ for case 2; (c) $\xi = 1$, $t = 1$ for case 3

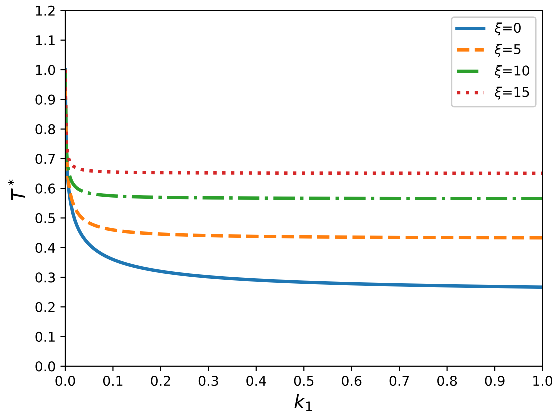

(a)

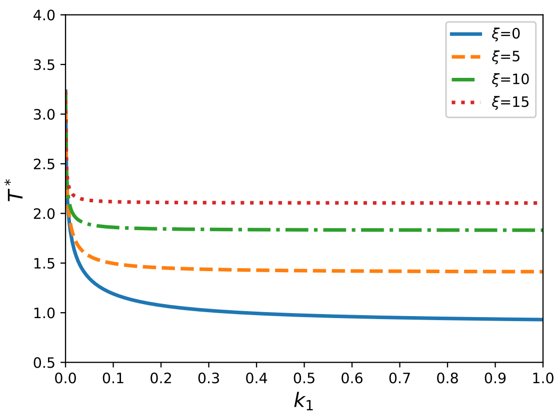

(b)

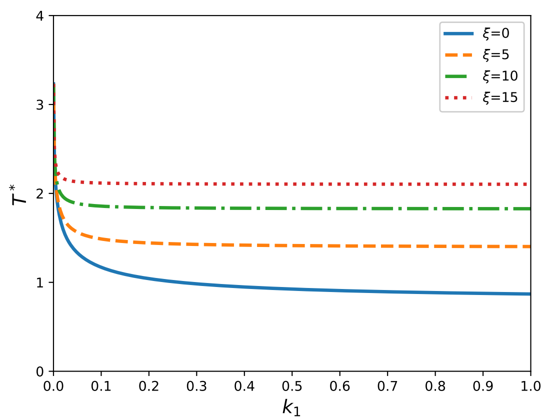

(c)

Fig. 6. Variation of torque versus permeability parameter with different values of Hartman number ξ: (a) $\beta_1 = 10$, $t = 1$ for case 1; (b) $\beta_1 = 10$, $t = 1$ for case 2; (c) $\beta_1 = 10$, and $t = 1$ for case 3

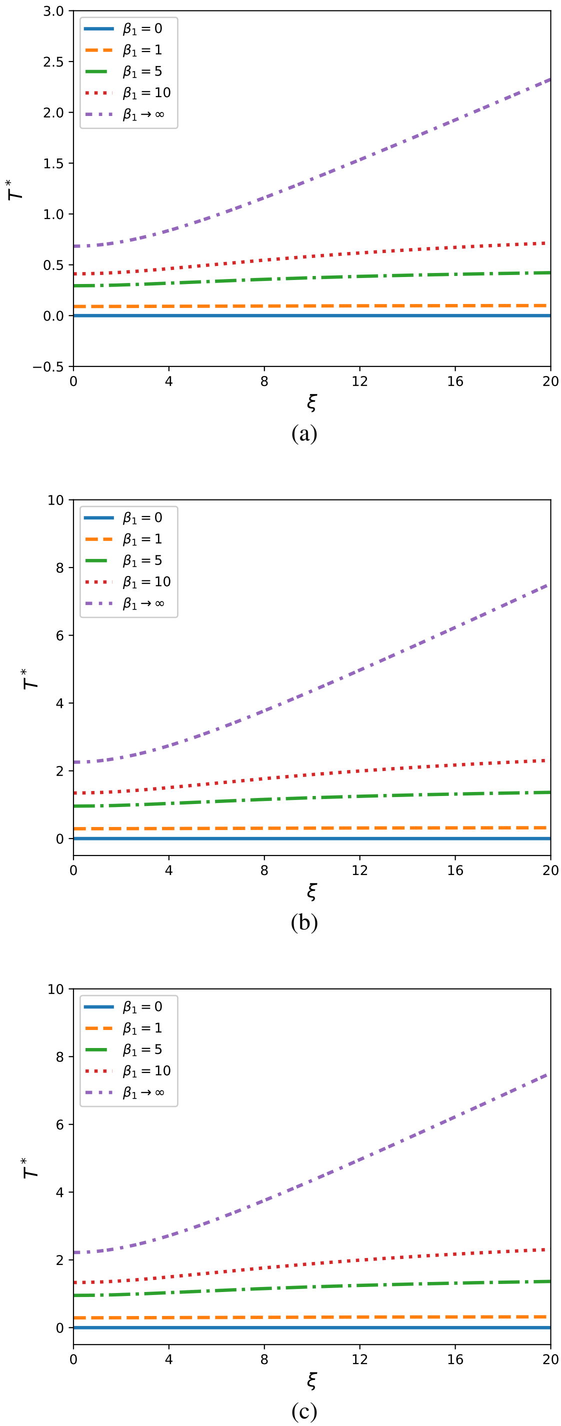

Fig. 7. Plots of torque versus Hartman number with different values of β_1 (a) $k_1 = 0.05$, $t = 1$ for case 1; (b) $k_1 = 0.05$, $t = 1$ for case 2; (c) $k_1 = 0.05$, $t = 1$ for case 3

6. Conclusions

In this study, the unsteady rotational motion of a rigid sphere in an axisymmetric, incompressible Newtonian fluid within a porous medium, with the presence of an applied magnetic field, is investigated. Expressions for the unsteady torque formula of the sphere in spherical polar coordinates is evaluated, which depend on the permeability parameter, Hartman number, and slip parameter. Three different fluid flows are discussed. The effects of the Hartmann number, permeability parameter, and slip parameter are represented graphically. We conclude that:

- Hartman number (ξ) and slip parameter (β_1) enhance the torque (T^*) experienced by the sphere for each cases.
- Torque (T^*) decreases with increasing values of the permeability parameter (k_1) for each cases.

Acknowledgements

One of the authors (Chitra Kumar) gratefully acknowledges the financial support provided by the Ministry of Social Justice and Empowerment, Government of India, under the National Fellowship for Other Backward Classes (NBCFDC Ref No.: 231610060100).

References

[1] H.C. Brinkman. A calculation of the viscous force exerted by a flowing fluid on a dense swarm of particles. *Applied Scientific Research*, 1:27–34, 1949. doi: 10.1007/BF02120313.

[2] J. Happel and H. Brenner. *Low Reynolds Number Hydrodynamics*, volume 1 of *Mechanics of Fluids and Transport Processes*. Springer, The Hague, 1983. doi: 10.1007/978-94-009-8352-6.

[3] F. Chorlton. *Textbook of Fluid Dynamics*. CBS Publishers and Distributors, New Delhi, 1985.

[4] D. Srinivasacharya and M.K. Prasad. Steady rotation of a composite sphere in a concentric spherical cavity. *Acta Mechanica Sinica*, 28(3):653–658, 2012. doi: 10.1007/s10409-012-0057-z.

[5] D. Srinivasacharya and M.K. Prasad. Rotation of a porous approximate sphere in an approximate spherical container. *Latin American Applied Researchl*, 45(2):107–112, 2015. doi: 10.52292/j.laar.2015.383.

[6] E.A. Ashmawy. Unsteady rotational motion of a slip spherical particle in a viscous fluid. *International Scholarly Research Notices*, 2012:513717, 2012. doi: 10.5402/2012/513717.

[7] E.A. Ashmawy. Unsteady Stokes flow of a couple stress fluid around a rotating sphere with slip. *The European Physical Journal Plus*, 131(5):175, 2016. doi: 10.1140/epjp/i2016-16175-6.

[8] P. Sarkar and K.P. Madasu. Impact of couple stresses on slow rotation of a slip sphere: Brinkman's medium. *International Journal of Applied and Computational Mathematics*, 10(3):116, 2024. doi: 10.1007/s40819-024-01749-x.

[9] C. Kumar and K.P. Madasu. Time-dependent rotational motion of a solid sphere in a Jeffrey fluid with velocity slip. *Physics of Fluids*, 37(8):083120, 2025. doi: 10.1063/5.0281800.

[10] C.Y. Chou and H.J. Keh. Slow rotation of a spherical particle in an eccentric spherical cavity with slip surfaces. *European Journal of Mechanics - B/Fluids*, 86:150–156, 2021. doi: 10.1016/j.euromechflu.2020.12.007.

[11] M.X. Li and H.J. Keh. Transient rotation of a spherical particle in a concentric cavity with slip surfaces. *Fluid Dynamics Research*, 53(4):045509, 2021. doi: 10.1088/1873-7005/ac1cd3.

[12] M. Ayman, E.I. Saad, and M.S. Faltas. Transient motion of a rotating slippery spherical particle within a spherical cavity filled with a porous medium. *Canadian Journal of Physics*, 103(7):638–653, 2025. doi: 10.1139/cjp-2024-0168.

[13] J.C. Maxwell. A dynamical theory of the electromagnetic field. *Philosophical Transactions of the Royal Society of London*, 155:459–512, 1865. doi: 10.1098/rstl.1865.0008.

[14] J. Hartmann. Theory of the laminar flow of an electrically conductive liquid in a homogeneous magnetic field. *Fysisk Meddelelser*, 15:1–27, 1937.

[15] W. Chester. The effect of a magnetic field on Stokes flow in a conducting fluid. *Journal of Fluid Mechanics*, 3(3):304–308, 1957. doi: 10.1017/S0022112057000671.

[16] R.V. Blerkom. Magnetohydrodynamic flow of a viscous fluid past a sphere. *Journal of Fluid Mechanics*, 8(3):432–441, 1960. doi: 10.1017/S0022112060000712.

[17] K. Gotoh. Magnetohydrodynamic flow past a sphere. *Journal of the Physical Society of Japan*, 15(1):189–196, 1960. doi: 10.1143/jpsj.15.189.

[18] F.A. Goldsworthy. Magnetohydrodynamic flows of a perfectly conducting, viscous fluid. *Journal of Fluid Mechanics*, 11(04):519–528, 1961. doi: 10.1017/s0022112061000706.

[19] S. Swarup and P.C. Sinha. Magnetohydrodynamic flow past a sphere. *Engineering Transactions*, 25(1):53–62, 1977.

[20] A.K. Singh and N. Kumar. Unsteady magnetohydrodynamic Couette flow. *Wear*, 89(2):125–129, 1983. doi: 10.1016/0043-1648(83)90237-5.

[21] G.S. Seth and S.K. Ghosh. Unsteady hydromagnetic flow in a rotating channel in the presence of inclined magnetic field. *International Journal of Engineering Science*, 24(7):1183–1193, 1986. doi: 10.1016/0020-7225(86)90013-3.

[22] P.K. Kythe and P. Puri. The effects of induced magnetic field on unsteady hydromagnetic flows in a rotating medium. *Astrophysics and Space Science*, 174(1):121–133, 1990. doi: 10.1007/bf00645658.

[23] T. Hayat, S. Asghar, A.M. Siddiqui, and T. Haroon. Unsteady MHD flow due to non-coaxial rotations of a porous disk and a fluid at infinity. *Acta Mechanica*, 151(1):127–134, 2001. doi: 10.1007/bf01272530.

[24] A.M. Siddiqui, M. Khan, S. Asghar, and T. Hayat. Exact solutions in MHD rotating flow. *Mechanics Research Communications*, 28(4):485–491, 2001. doi: 10.1016/s0093-6413(01)00199-9.

[25] T.V.S. Sekhar, R. Sivakumar, and T.V.R.R. Kumar. Magnetohydrodynamic flow around a sphere. *Fluid Dynamics Research*, 37(5):357–373, 2005. doi: 10.1016/j.fluiddyn.2005.08.003.

[26] P.K. Kythe and P. Puri. Unsteady MHD free-convection flows with time-dependent heating in a rotating medium. *Astrophysics and Space Science*, 135(2):219–228, 1987. doi: 10.1007/bf00641556.

[27] S. Chandrasekhar. The stability of viscous flow between rotating cylinders in the presence of a magnetic field. *Proceedings of the Royal Society of London A*, 216(1126):293–309, 1953. doi: 10.1098/rspa.1953.0023.

[28] P. Puri and P.K. Kulshrestha. Unsteady hydromagnetic boundary layer in a rotating medium. *Journal of Applied Mechanics*, 43(2):205–208, 1976. doi: 10.1115/1.3423809.

[29] C. Geindreau and J.L. Auriault. Magnetohydrodynamic flows in porous media. *Journal of Fluid Mechanics*, 466:343–363, 2002. doi: 10.1017/S0022112002001404.

[30] P. Saxena and A.C. Srivastava. Rotation of a solid sphere in a viscous fluid bounded by a concentric spherical porous medium. *Journal of Porous Media*, 11(6):575–588, 2008. doi: 10.1615/JPorMedia.v11.i6.50.

[31] P. Saxena and M. Agarwal. A study of the effect of transverse magnetic field on the rotation of a solid sphere in a viscous fluid bounded by a concentric spherical porous medium. *Special Topics & Reviews in Porous Media: An International Journal*, 7(1):1–13, 2016. doi: 10.1615/specialtopicsrevporousmedia.v7.i1.10.

[32] S. Das, S.L. Maji, M. Guria, and R.N. Jana. Unsteady MHD Couette flow in a rotating system. *Mathematical and Computer Modelling*, 50(7–8):1211–1217, 2009. doi: 10.1016/j.mcm.2009.05.036.

[33] G.S. Seth, M.S. Ansari, and R. Nandkeolyar. Effects of rotation and magnetic field on unsteady Couette flow in a porous channel. *Journal of Applied Fluid Mechanics*, 4(2):95–103, 2011. doi: 10.36884/jafm.4.02.11922.

[34] A.R. Premlata and H.-H. Wei. History hydrodynamic torque transitions in oscillatory spinning of stick-slip Janus particles. *AIP Advances*, 9(12):125113, 2019. doi: 10.1063/1.5131678.

[35] G. Nagaraju, K. Kaladhar, and K.S. Sai. Magnetohydrodynamics effect on rotating free surface flow of micropolar fluid in a cylindrical container with porous lining. *International Journal of Dynamical Systems and Differential Equations*, 5(3):191–205, 2015. doi: 10.1504/ijdsde.2015.071001.

[36] K.P. Madasu and T. Bucha. Effect of magnetic field on the slow motion of a porous spheroid: Brinkman's model. *Archive of Applied Mechanics*, 91(4):1739–1755, 2021. doi: 10.1007/s00419-020-01852-7.

[37] K.P. Madasu and T. Bucha. Creeping flow of fluid sphere contained in a spherical envelope: magnetic effect. *SN Applied Sciences*, 1(12):1594, 2019. doi: 10.1007/s42452-019-1622-x.

[38] K.P. Madasu and T. Bucha. Influence of MHD on micropolar fluid flow past a sphere implanted in porous media. *Indian Journal of Physics*, 95(6):1175–1183, 2020. doi: 10.1007/s12648-020-01759-7.

[39] S. El-Sapa and N.S. Alsudais. Effect of magnetic field on the motion of two rigid spheres embedded in porous media with slip surfaces. *The European Physical Journal E*, 44(5):68, 2021. doi: 10.1140/epje/s10189-021-00073-2.

[40] S. El-Sapa. The force on a magneto-spherical particle oscillating in a viscous fluid perpendicular to an impermeable planar wall with slippage. *European Journal of Pure and Applied Mathematics*, 15(3):1376–1401, 2022. doi: 10.29020/nybg.ejpam.v15i3.4442.

[41] A. Al-Hanaya and S. El-Sapa. Impact of slippage on the wall correction rotation factor of MHD couple stress fluid between two concentric spheres. *Results in Engineering*, 20:101463, 2023. doi: 10.1016/j.rineng.2023.101463.

[42] M.A. Alotaibi and S. El-Sapa. MHD couple stress fluid between two concentric spheres with slip regime. *Results in Engineering*, 21:101934, 2024. doi: 10.1016/j.rineng.2024.101934.

[43] P.K. Yadav, M. Roshan, and A.N. Filippov. A hemodynamic perspective to analyze the pulsatile flow of Jeffrey fluid through an inclined overlapped stenosed artery. *Colloid Journal*, 86(4):627–643, 2024. doi: 10.1134/S1061933X24600349.

[44] P.K. Yadav and M. Roshan. Heat transfer analysis of a peristaltically induced creeping magnetohydrodynamic flow through an inclined annulus using homotopy perturbation method. *ZAMM - Journal of Applied Mathematics and Mechanics / Zeitschrift für Angewandte Mathematik und Mechanik*, 104(11):e202400198, 2024. doi: 10.1002/zamm.202400198.

[45] P.K. Yadav and M. Roshan. Mathematical modeling of blood flow in an annulus porous region between two coaxial deformable tubes: An advancement to peristaltic endoscope. *Chinese Journal of Physics*, 88:89–109, 2024. doi: 10.1016/j.cjph.2024.01.017.

[46] P.K. Yadav and M. Roshan. Mathematical modeling of creeping electromagnetohydrodynamic peristaltic propulsion in an annular gap between sinusoidally deforming permeable and impermeable curved tubes. *Physics of Fluids*, 36(7):071907, 2024. doi: 10.1063/5.0217370.

[47] P.K. Yadav and M. Roshan. Effect of peristaltic endoscope and heat transfer on the magnetohydrodynamic flow of non-Newtonian biviscosity fluid through an inclined annulus: Homotopy perturbation approach. *Modern Physics Letters B*, 39(14):2450498, 2025. doi: 10.1142/S0217984924504980.

[48] C.P. Moerland, L.J. von IJzendoorn, and M.W.J. Prins. Rotating magnetic particles for lab-on-chip applications – a comprehensive review. *Lab on a Chip*, 19(6):919–933, 2019. doi: 10.1039/c8lc01323c.

[49] G. Cai, Z. Yang, Yu-C. Chen, Y. Huang, L. Liang, S. Feng, and J. Zhao. Magnetic bead manipulation in microfluidic chips for biological application. *Cyborg and Bionic Systems*, 4:0023, 2023. doi: 10.34133/cbsystems.0023.

[50] J.F. Liu, B. Jang, D. Issadore, and A. Tsourkas. Use of magnetic fields and nanoparticles to trigger drug release and improve tumor targeting. *WIREs Nanomedicine and Nanobiotechnology*, 11(6):e1571, 2019. doi: 10.1002/wnan.1571.

[51] R. Moreau. *Magnetohydrodynamics*. Springer Dordrecht, 1990. doi: 10.1007/978-94-015-7883-7.

[52] E.A. Ashmawy. Rotary oscillation of a composite sphere in a concentric spherical cavity using slip and stress jump conditions. *The European Physical Journal Plus*, 130(8):163, 2015. doi: 10.1140/epjp/i2015-15163-8.

[53] K.P. Madasu and P. Sarkar. Torque on the slow rotation of a slightly deformed slip sphere in a Brinkman medium. *Pramana*, 97(1):44, 2023. doi: 10.1007/s12043-022-02505-w.

[54] Y.E. Solomentsev and J.L. Anderson. Rotation of a sphere in Brinkman fluids. *Physics of Fluids*, 8(4):1119–1121, 1996. doi: 10.1063/1.868890.

[55] A. Talbot. The accurate numerical inversion of Laplace transforms. *IMA Journal of Applied Mathematics*, 23(1):97–120, 1979. doi: 10.1093/imamat/23.1.97.

[56] A. Murli and M. Rizzardi. Algorithm 682: Talbot's method for the Laplace inversion problem. *ACM Transactions on Mathematical Software*, 16(2):158–168, 1990. doi: 10.1145/78928.78932.

[57] A.M. Cohen. *Numerical Methods for Laplace Transform Inversion*. Springer, New York, 2007.

[58] E.I. Saad. Effect of magnetic fields on the motion of porous particles for Happel and Kuwabara models. *Journal of Porous Media*, 21(7):637–664, 2018. doi: 10.1615/jpormedia.v21.i7.50.

[59] P.K. Maurya, S. Deo, and D.K. Maurya. Couple stress fluid flow enclosing a solid sphere in a porous medium: Effect of magnetic field. *Physics of Fluids*, 35(7):072006, 2023. doi: 10.1063/5.0155532.